International Academic Institute for Science and Technology

International Academic Journal of Science and Engineering
Vol.10, No.1, 2023, pp.20-26.

ISSN 2454-3896

International Academic Journal of Science and Engineering

www.iaiest.com

The Effectiveness of TiO2 Thermal Barrier Coating in Protecting IN738 LC Super Alloy in an Atmosphere of Sodium Sulfate and Sodium Chloride Vapor at High Temperature

Mahmood Ahmed Hamood [a]

[a] *Department of Physics, College of Sciences, University of Mosul, Iraq.*

Abstract

Increasing the efficiency of work and extending the life of metal equipment, which operates under very harsh conditions, requires making the best complex changes in its crystalline structure and properties. In many of the properties of this equipment as a result of the formation of multi-layered metal and ceramic layers in the surface construction of the ingot, thus increasing the efficiency of the ingot and extending its life. The aluminizing was carried out in the presence of a thermal barrier yttrium oxide at 1000 oC, and the oxidation kinetics of the coated structures was studied at 1050 oC and in an atmosphere of mixture sodium chloride vapor and sodium sulfate.

Keywords: Hot Corrosion, TBC of Super Alloys, High Temperature Oxidation, Pack Cementation.

DOI:10.71086/IAJSE/V10I1/IAJSE1004
Received: 15 December 2022/Revised: 14 January 2023/Accepted: 20 February 2023/Published: 30 March 2023

Introduction

Engines need structural materials with a high melting point, especially for high pressure turbines (HPT), where nickel-based super alloys are an inevitable material for the manufacture of discs and turbine blades. This is due to its excellent physical chemical, and mechanical properties, even under the harsh conditions in which it operates. of different mechanisms [3,4]. But even in air, the oxidation resistance of the improved nickel-cobalt-based alloys is not sufficient for continuous operation above 1000 °C [5]. The growth of the oxide Enhanced alloys is operated in industrial environments containing various types of corrosives such as sulfates, chlorides or carbon-containing compounds, water vapor, alkali and alkaline earth metal salts [1,2]. When operating this equipment at high temperatures, these compounds cause a wide range of types of attack on most metal alloys such as oxidation, Carbonization, vulcanization, hot corrosion, or a combination crust very quickly and the structural changes of the substance surface region of the alloy loses its mechanical strength [6-8]. Developments and improvements in industrial technology have led to more efficient large additions of alloying elements such as chromium, aluminum, silicon Cr, Al or Si because they lead to a loss in some mechanical properties such as fatigue and resistance Tensile and creep resistance operations and more powerful engines with an increase in operating temperatures, and this is done by not using, as well as leads to brittleness of the product and a decrease in its melting point at high temperature [9, 10, 11]

Therefore, the only way to overcome this problem is to apply high temperature diffusion coatings to counter aggressive corrosive high temperature atmospheres and make possible processes that cannot be operated efficiently and reliably without such coatings.

Diffusive coatings are used to protect the system from oxidation and corrosion [12]. Besides protection against oxidation and corrosion, the other major factor affecting the overall lifespan of substrates at high temperatures is the effects of heat flux. The diffusion layers that appear in the coating, including the ceramic layer in the highest formation of the thermal barrier coating system, constitute the first barrier to attack by the environment [13]. The idea behind all oxidation and corrosion resistant diffusion coatings is to create a reservoir of active ingredients that react with the surroundings to form oxides with good thermal insulators and a high melting point through which to form a dynamically and thermally stable, slow growing, adherent oxide crust consisting of corrosion products, usually oxide. It grew thermally on the surface.

The harsh operating conditions often generate defects such as cracks even with the presence of stable protective oxide scales, and thus requires the alloy to be able to reshape these oxides for self-defense and get rid of cracks through the formation of ceramic layers and oxide layers that grow thermally slowly and form several oxide scales times before the protective coating element tank is exhausted [14,15,16].

Experiment Technique

Here we discuss the design and manufacture of special ovens for conducting hot corrosion tests to test the metal and the used coatings, the design and manufacture of the coating system, which includes aluminized crucible , and the oven for coating, how to connect the coating system to the vacuum system, and a description of all the devices used, and this part includes the entirety of the experiments that Conducted within the requirements of the research preparation and coating methods that were followed in this Research, as well as hot corrosion tests of coated and uncoated samples which are carried out in the factory oven.

As for the examinations that took place during this work, they included microscopic examination of the samples before and after coating and before and after the corrosion test. Surface analysis of the samples was carried out using the X-ray diffraction device (XRD) after coating the samples, as well as after conducting the corrosion tests. The samples were photographed with the usual optical microscope. Finally, the samples were taken. The coated and corrosion surface analysis of the samples was performed using a scanning electron microscope (SEM - EDX) to accurately determine the coating elements present through the layers of coatings and corrosion, and supported the examinations with an X-ray diffraction device, and the thickness of the coating was measured with a device type (AHSLER Type V- Testor 2).

The composition of IN738LC alloy under work is in table (1)

Table 1: Composition of the IN738LC Superalloy

Component	Cr	Ni	Co	Fe	W	Mo	Ti	Al	C	Nb	Zr	Ta
Wt%	15.8	BAL	8.6	0.04	2.7	1.8	3.3	3.6	0.1	0,8	0.04	1.8

Pack Cementation

It is one of the methods of diffusion coating, and the cementation process was carried out for all the samples prepared and for the various alloys that were dealt with in the research using a cement mortar consisting of a powder that contains the powder of the coating material, and here the coating material is aluminum by (25%), and aluminum chloride powder by (5.6%) as an activator And aluminum oxide (alumina) at a rate of (69.4%) as a substance that helps prevent agglomeration of the mixture, and the mixture is mixed well and the sample to be coated is placed inside the powder and closed well from the open end and placed inside the tube inside the furnace and connected from its open end to the vacuum device, and the temperature of the furnace is fixed At the required temperature, which is (1000 ºC), and the cementation process continues for (4, 8, 16) hours.

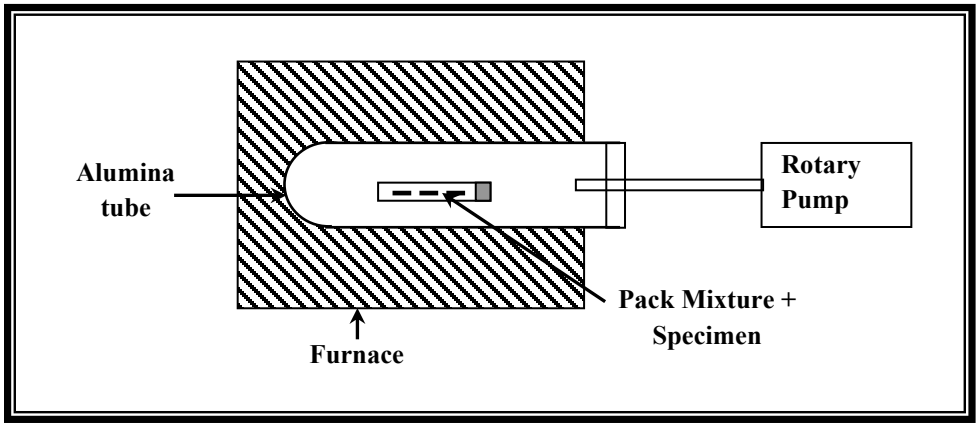


Fig. 1: The Figure Shows the Coating System Used in this Research

Microscopic Examination and Imaging of Samples

After completing the coating and hot corrosion tests, the samples are subjected to cold-amounting operations, and then grinding operations are performed using smoothing paper made of silicon carbide of granular size (220, 320, 400, 1200) and then polishing using diamond paste or alumina solution (Diamond Paste), and then washed with water and washing powder, then with alcohol, and finally dried to move to the etching stage, in which three types were used of the solutions are:

1. Nital solution, which consists of nitric acid (2% HNO3) and ethyl alcohol or absolute (pure) methyl alcohol (Absolute al) (98%)
2. Keller's solution consists of hydrofluoric acid (0.5% Hf), hydrochloric acid (1.5% Hcl) and nitric acid

Aluminizing the Nickel-Iron based Alloy (IN738) in the Presence of a Thermal Barrier (TiO2)

From the observation of the coating layer in Figure (2), which was obtained from the microscopic examination after completing the surface finishing operations, we find that the coating layer consists three layers characterized by the presence of a thick outer and inner layer and contains a high density of sedimentation of fine grain size and others as secondary phases They differ in their effect with the solution of appearance, and this is clear from the figure(2)

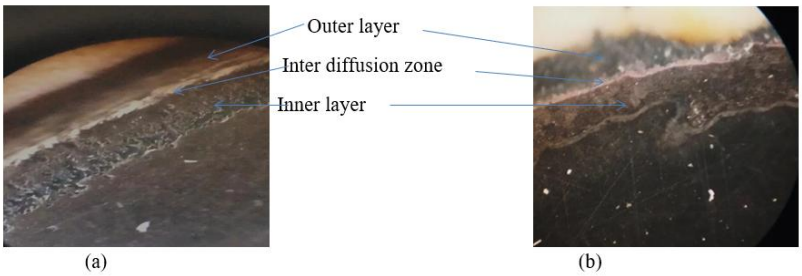


Fig. 2: Microstructure of the Super Alloy 738LC Aluminizing in the Presence of Titanium Oxide as Thermal Barrier (a:4h, b: 8h)

The outer layer (Outer layer) based on the phase (NiAl), and its thickness increases with the increase of the coating time, and it can be distinguished between them through the density of sediments, secondary phases, and the particle size of this region Which contains deposits as aluminum-chrome phases in the middle and inner regions, according to their different densities. As for the inner layer has a poly phases appearance and is phase-based (Ni3Al) and show free from sedimentation, as shown by the highlighting solution itself, and this structural structure is repeated with increasing coating time and with greater thickness. The inter diffusion zone it is characterized by a light-yellow color and is almost free of sedimentation.

The topography of the surface was examined by a scanning electron microscope. As in the figure, we find that for the diffusion coating for a period of four hours, there are needle structures that belong to the nickel-aluminum phase, in addition to other structures of the alumina phase, the aluminum-iron phase, and the iron-nickel phase. In the case of the diffusion coating for an eight-hour period, these structures disappeared. The needles became spherical structures and belonged to the same phases, but with different concentrations, and as clearly shown at 500 nm magnification. Fig (3).

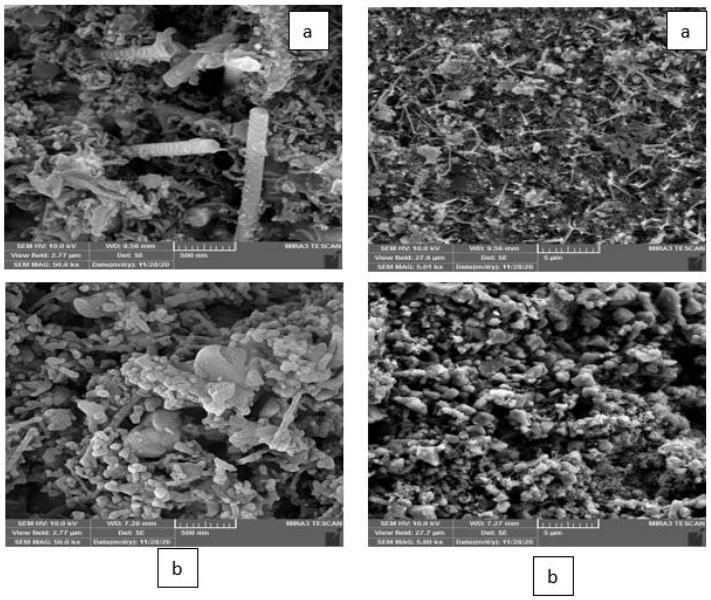


Fig. 3: SEM Plan View Picture, Showing a Alumina Needles are Observed, Covering the Majority of the Surface for a: 4h TBCs, and Spherical at b: 8h TBCs

This analysis confirmed the X-ray diffraction examination, which confirmed the presence of these phases by calculating the Miller coefficients and the intensity of the peaks at two theta and comparing them with the ICDD card, as shown in the following figures 4 and 5.

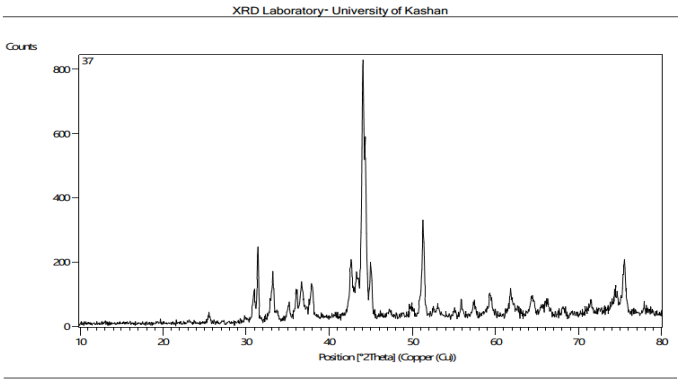


Fig. 4: XRD Analysis of Sample Aluminized 4h

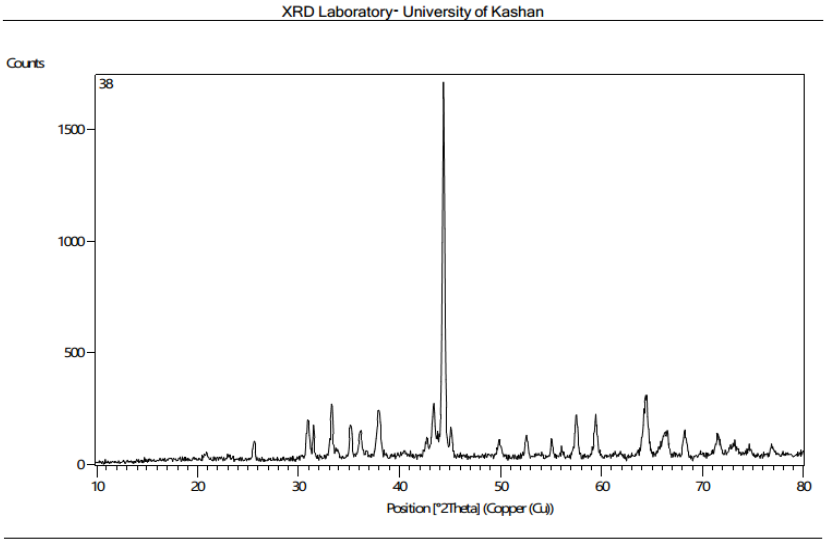
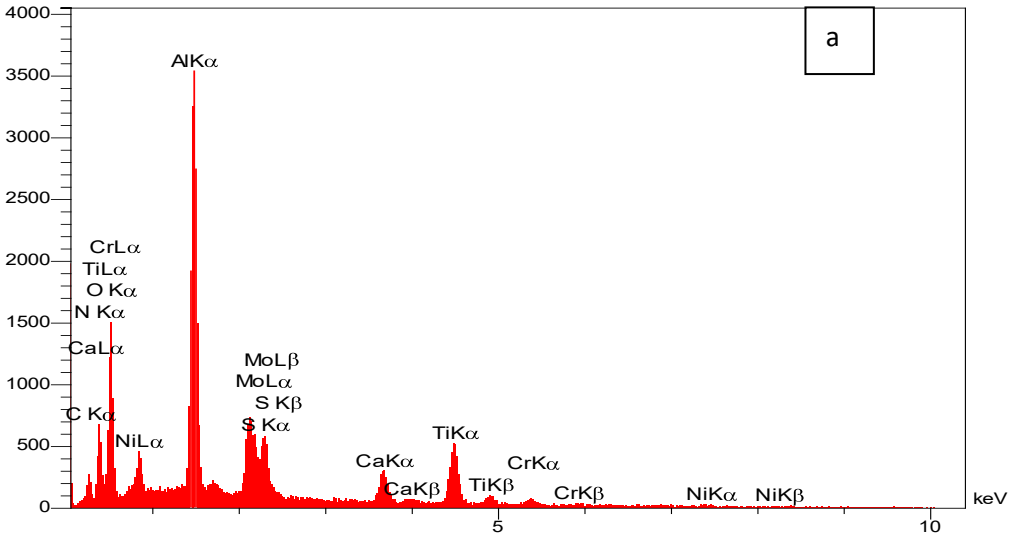


Fig. 5: XRD Analysis of Sample Aluminized 8h

The results of the X-ray spectrum analysis, Figure (5), showed the presence of the basic and stable phase (NiAl), and it was not possible to confirm the presence of the (FeAl) phase because these two phases have the same crystalline structure and it is not easy to distinguish between them using X-rays.

The alloy contains (18.5%wt) iron, so it is not excluded that phases will form Iron-aluminum as secondary phases rich in aluminum such as (Fe_4Al_{13}), which actually appeared using X-ray examination, and the presence of chromium (19% wt) and solubility in the compound. The medium (NiAl) is not more than (5%wt) making chromium-aluminum compounds predominate as precipitating phases through the coating layer, in addition to phases that are difficult to identify and may result from the combination of the element columbium originally present in the alloy at a ratio of (5.1%wt)) with plating elements (aluminum and yttrium). In general, the microscopic examination, which shows many phases and their different colors, has been expressed by the complexities resulting from the analysis of the X-ray results (Table 2).



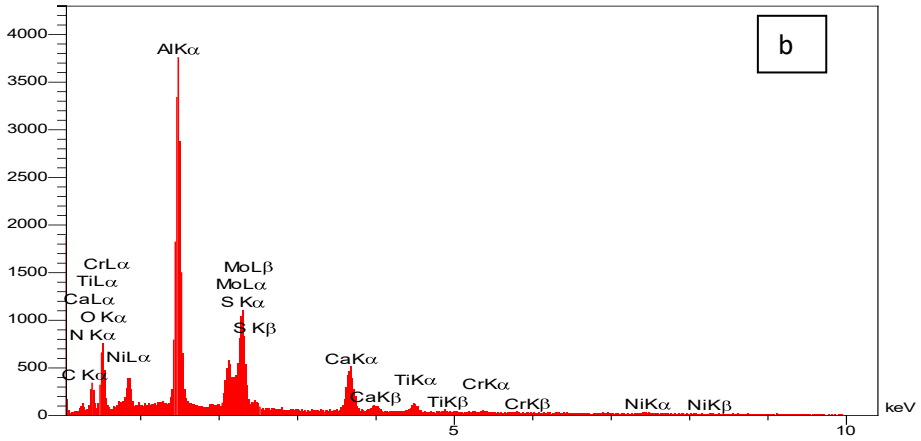


Fig. 6: Quantitative and Qualitative of TBC of IN738 LC at a: 4h, b: 8h

Table 2: X-ray Diffraction (XRD) Results for the Enhanced Type Alloy (IN738LC) Painful in the Presence of a Thermal Barrier (Y2O3)

Peak No.	R.Int(I/I₀)	d ºA	2Θ	Phase type.
1	7%	4.147	22.3	Ã
2	7%	3.465	26	Ã
3	16%	2.888	31	□,⌂
4	16%	2.570	34	◊,*, ♠
5	27.5%	2.281	38.5	♠,♀,∂,♣
6	26%	2.116	42.5	◊, ☺,*, ♀,∂
7	100%	2.051	44.0	□,♀,☺,⌂ , ∂,♣
8	64%	2.020	45	□,∂
9	12%	1.900	47	□, ◊, ☺,*,∂ , ♠,♣
10	13%	1.772	51.5	◊, *,∂, ♠
11	13%	1.669	50	□,⌂,♠
12	19%	1.609	57	♠,♣
13	20%	1.445	64.3	◊,♀, ☺,*,⌂,∂,♠
14	13%	1.411	66.0	□, ◊,∂, ♠
15	10%	1.378	67.8	◊,∂
16	16%	1.243	76.5	◊, ☺, *, ♀,♣
NiAl=□	**$CrAl_2$ =♀**	**$CrAl_5$=◊**	**Cr_3Al_2=***	**Cr_5Al_8=☺**
FeAl = ⌂	**Fe_4Al_{13} =∂**	**$TiAl_3$=♠**	**TiO_2=♣**	

It was noted by visual examination that the protective oxide layer (Al_2O_3) remained while it was still attached to the paint layer. It was tried to extract it at the end of the exposure period without success, and although this crust suffered from bulges in areas on the surface of the model, it did not suffer from precipitation during thermal cycles due to thermal stresses. Where the image showed fine details of the coating layer. It clearly showed the emerging fractures of the protective oxide layer.

Clearly, cracks arising from the protective oxide layer and areas of its separation from the coating caused by some precipitation. It is worth noting the presence of carbide deposits, perhaps chromium, titanium and molybdenum carbides, in the separating area between the alloy and the coating, i.e. below the coating layer, which was deposited due to the limited solubility of chromium in the coating layer, the quantitative and qualitative analysis of the elements by the SEM-EDAX device, Figure (5,6) and Table (2), showed that it contained (32wt%) of aluminum and (57wt%) of nickel. The proportions correspond to the composition of the phase (NiAl) rich in nickel (Ni-rich NiAl). It is also noted that the percentage of both iron and chromium elements in this layer has decreased significantly, as the percentage of chromium has become (3.8wt%), which is actually less than (5wt%), i.e. permissible percentage in the phase (NiAl). The corrosion kinetics curve (mass change with time) Figure (6) confirms good stability throughout the time period and this due to good adhesion of the protective layer. It seems that these results are consistent with the observations of a number of researchers. Where the TBC coating proved to have excellent stability for 8 hours, exceeding 300 hours without any change in weight, while the TBC models for two hours and the non- TBC models began to change in weight after 230 hours, and for the TBC models for four and six hours, a

slight change in weight began after 100 hours, then stability was observed to the 67th session, that is, after 230 hours of severe testing.

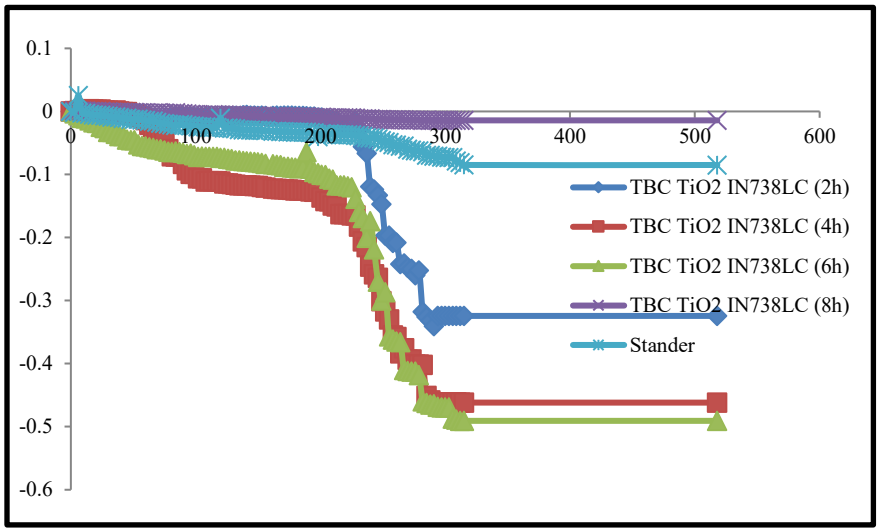


Fig. 6: Weight Loss Per Unit Area Against Time

Conclusion

Through this work, it was found that the diffusion coating with thermal barrier coating TBC, titanium oxide, on the super alloy at the times of 2, 8 hours is highly efficient in resisting hot corrosion, while we show through Figure 4 that the TBC with the times of 4,6 hours are less efficient.

References

Reed. R.C. (2006). The Super alloys: Fundamentals and Applications, Cambridge University Press, 283-335.

Subramanian, R., Burns, A., & Stamm, W. (2008). Advanced multi-functional coatings for land-based industrial gas turbines. In *Turbo Expo: Power for Land, Sea, and Air*, *43116*, 549-558.

Young, D.J. (2008). *High temperature oxidation and corrosion of metals*, *1*, 139-455.

Kofstad. P. (1988). High Temperature Corrosion, Essex UK: Elsevier Applied Science. 139-181.

Vialas, N., & Monceau, D. (2006). Substrate effect on the high-temperature oxidation behavior of a Pt-modified aluminide coating. Part I: influence of the initial chemical composition of the coating surface. *Oxidation of Metals*, *66*, 155-189.

Dryepondt, S., Monceau, D., Crabos, F., & Andrieu, E. (2005). Static and dynamic aspects of coupling between creep behavior and oxidation on MC2 single crystal superalloy at 1150 C. *Acta materialia*, *53*(15), 4199-4209.

Seetharaman, V., & Cetel, A.D. (2004). Thickness debit in creep properties of PWA 1484. *Superalloys*, 207-214.

Srivastava, A., Gopagoni, S., Needleman, A., Seetharaman, V., Staroselsky, A., & Banerjee, R. (2012). Effect of specimen thickness on the creep response of a Ni-based single-crystal superalloy. *Acta Materialia*, *60*(16), 5697-5711.

Heilmaier, M., Kreger, M., Saage, H., Rösler, J., Mukherji, D., Glatzel, U., & Burk, S. (2009). Metallic materials for structural applications beyond nickel-based superalloys. *Jom*, *61*, 61-67.

Hamood, M. (2023). The effectiveness of TiO_2 thermal barrier coating in protecting IN738 LC super alloy in an atmosphere of sodium sulfate and sodium chloride vapor at high temperature. *International Academic Journal of Science and Engineering, 10(1)*, 20–26. https://doi.org/10.71086/IAJSE/V10I1/IAJSE1004

Sims, C.T. (1984). A history of superalloy metallurgy for superalloy metallurgists. *Superalloys*, *1984*, 399-419.

Goward, G.W. (1998). Progress in coatings for gas turbine airfoils. *Surface and coatings technology*, *108*, 73-79.

Clarke, D.R., Oechsner, M., & Padture, N.P. (2012). Thermal-barrier coatings for more efficient gas-turbine engines. *MRS bulletin*, *37*(10), 891-898.

Hamood, M. A., & Abed, M. A. (2012). Oxidation study of cobalt-base super alloys at high temperatures in molten salt of Na2SO4. *Rafidain Journal of Science*, *23*(7), 127-136.

Hamood, M., Mahmood, R., & Edrees, E. (2018). The use of Dy_2O_3 as thermal barrier in aluminide coating on one type of stainless steel. *Rafidain Journal of Science, 27(1),* 125–134.

Salman, Y.A., Hmood, M.A., & Ghadeer, E.E. (2020). The Effect of Nickel and Aluminum Concentration on Cyclic Oxidation Resistance of Mild Steel (AISI 1020). *Journal of Education and Science*, *29*(3), 1-10.